Vietnam Journal of Catalysis and Adsorption
Tạp chí xúc tác và hấp phụ Việt Nam

https://chemeng.hust.edu.vn/jca/

Synthesis of metal organic framework mesostructured UIO-66 with defections in frameworks for enhancing photocatalytic degradation of residues pesticides

Nguyen Duc Hai[1,2], Vũ Minh Tan[1], Nguyen Thi Thu An[3], Phuong Long Ha[3], Hoang Mai Ha[3], Hac Thi Nhung[3], Ho Thi Oanh[3], Nguyen Duc Tuyen[3], Nguyen Quyet Tien[3], Nguyen Quảng An[3], Nguyen Ngoc Tuan[3], Nguyen Dinh Tuyen[2,3*]

[1]*Hanoi University of Industry, Hanoi, Vietnam*
[2]*Graduate University of Sciences and Technology, Vietnam Academy of Science and Technology, Hanoi, Vietnam*
[3]*Institute of Chemistry, Vietnam Academy of Science and Technology, Hanoi , Vietnam*
**Email: tuyenndvast@gmail.com*

ARTICLE INFO

Received: 15/5/2021
Accepted: 25/6/2021
Published: 15/10/2021

Keywords:

Defected mesostructured UiO-66, photocatalytic degaradation, chlorpyrifos ethyl pesticide

ABSTRACT

Novel photocatalysts, based on modified mesostructured UiO-66-Zr composites with defects sites in framewwork arrays were prepared by solvothermal synthesis method using CTABr as ionic surfactant template, acetic acid and benzoic acid as modulators. Modified UiO-66-Zr with defects sites in framewworks by using ionic surfactants CTABr, benzoic acid (UiO-66-M) and acetic acid (UiO-66-A) as modulators were synthesized, characterized by BET, XRD, FTIR, TEM, EDX techniques. The photocatalytic performances over material samples were tested in photodegradation of chlopyrifos ethyl in aqueous solution under simulated solar light irradiation and evaluated by UV-Vis spectra commbied with HPLC analysis. These modified UiO66 showed a highly effective photodegradation and mineralization of chlopyrifos ethyl (peesticide/insecticide) in aqueous solution. The photocatalytic activities of the modified UiO66-Zr were considerably greater than unmodified UiO66-Zr composites were explained by the roles of defected sites created in material framewworks. The presence of the defects not only resulted in the dramatically enhanced porosity (pore size), but also induced the creation of Zr-OH groups which served as the main active adsorption sites for efficient ROS sequestration.The photo-degradation rate of chlopyrifos ethyl was ranked in the order of samples UiO66-Zr-M > UiO66-Zr-A > UiO66-Zr with reaction constant rate of k_3 = 1.23×10^{-2} (min^{-1}) > k_2 = 9.1×10^{-3} (min^{-1}) > k_1 = 2×10^{-4} (min^{-1}), respectively. The obtained results showed potential application of modified UiO66-Zr composites for photocatalytic treament of hydrophobic pesticide residues in water without any toxic secondary pollution in agriculture.

Introduction

Environmental agriculture pollutions by pesticies in soil, water, and air are affecting more adversely to human life all over the world. Study on treatment and removal of pollution compounds, especially toxic organic compounds in aqueous solutions is thus important and urgent. Pesticide is a generic

https://doi.org/10.51316/jca.2021.139

term that covers a wide range of biologically-active compounds, including herbicides, fungicides and insecticides which were used in agicultures.[1] Chlopyrifos ethyl have been used worldwide on a large scale in agriculture to control the growth of broad-leaved weeds on rice, maize, fruit vegetable and in post-emergence applications in most developing countries.[1,2] There are many techniques to reduce and degradation of chlopyrifos reesidues, namely thermal desorption, biological method, photochemical catalysis, adsorption and liquid phase extraction.[2] Among these methods, adsorption and photocatalysis methods have been widely studied due to low operating cost, easer of handling and high efficiency. Metal-organicframeworks (MOFs) are an emerging class of porous crystalline materials that consist of organic linkers and inorganic nodes. They have been widely studied due to their fundamental importance and versatile application potential, such as gas separation and catalysis, sensing devices, ion exchange, etc.[2,5] Since finding out, great number of reseachs have been taken to tailor various aspects of MOF, including the introduction of functional groups to the linker, particle size control, attaching one or more metal cores into the framework, and engineering the number of missing linker and/or missing cluster defects. To be specific, the most hydrothermal stable metal–organic frameworks containing zirconium UiO-66 are crystal materials that consist of organic linkers H_2BDC and zirconium as inorganic nodes.[4,5] UiO-66 crystals have large surface area but their pore size are small (1.5-2.5 nm) which limited in applications. The highly ordered mesoporous UiO66-Zr material was synthesis normally by using soft template as ionic surfactant (CTABr) [3]. Mesostructured UiO-66 possess uniform and large pore size, which enables bulky molecules to diffuse easily and contact with the active centers in the pore [3-7]. These materials can be also modified by creation defect sites (missing linker) in framework by using acetic acid and benzoic acid as modulators [8-10]. Due to their structure these materials can significantly facilitate the transfer of photocarriers and suppressed the recombination of photogenerated electrons/holes and increase quantum efficency in photocatalytic degradation of organic pesticides such as hydrophobic Chlopyrifos ethyl [8-14].

In this study, we focused on synthesizing modified MOFs material with defects creation in mesoporous UiO66-Zr structure. The defects can narrow the band gap of UiO-66, and this is majority attributed to the density of unrecombination electron/hole paires flow under light irradiation. These modified MOFs material acts as novel photocatalyst that promotes the photo oxidation degradation of chlopyrifos ethyl in aqueous solution under irradiation of UV light and simulated solar light.

Experimental

Chemicals

Benzen-1,4-dicacbonxylic acid (H_2BDC) (Sigma Aldrich, 99.5 %), Zirconyl chloride octahydrate ($ZrOCl_2.8H_2O$, Sigma Aldrich, 98 %), NN-dimethylformamide(DMF)$(CH_3)_2NC(O)H$,China,99%),Hexadecyl-trimethyl-ammoniumbromide CTABr)$(H_3C-(CH_2)_{15}-N+(CH_3)_3$ (Br-), Merck, 98 %), acetic acid (CH_3COOH, China, 99.5 %), Hydrochloric acid (HCl, China, 36.5 %), Sodium hydroxide (NaOH, China, 98 %), Benzoic acid (C_6H_5COOH, England) 98 %), toluene ($C_6H_5CH_3$, Chiana, 99.5 %), ethanol (C_2H_5OH, China, 96 %) Methylen blue (Sigma Aldrich), Methanol (China), Chlopyrifos ethyl (99.95 %, Analysis trade standar from Sigma).

Preparation

Synthesis of modified UiO-66

Typical, $ZrOCl_2.8H_2O$ (6.44 g), H_2BDC (3.32 g), 36 % HCl (5ml) were dissolved in 280 ml DMF with the assistance of ultrasonication for 30 minutes. Subsequently, the mix was transferred into a Teflon-autoclave, sealed and placed in a preheated oven at 120 ^oC for 24 hours. After cooling down to room temperature, the pre-cipitate was collected by centrifugation and washed with DMF three times. Then the solid was stirred in DMF at 363 K for 12 h, then in methanol at 333 K for 12 h to remove unreacted chemicals and solvent. The resulting white powder was dried under vacuum at 423 K for 12 h.

Synthesis of modified UiO-66 using acetic acid (UiO-66-Zr-A)

$ZrOCl_2.8H_2O$ (2.00 g), 99.5 % acetic acid (40ml) was dissolved in 700 ml DMF, ultrasonicated for 30 minutes, heated at 130 ^oC for 2 hours. After that 7.5 g added of H_2BDC the mix was stirred for 18 hours at 25 ^oC. The resulting mix was filtered, washing several times, and

purified with DMF and ethanol for removal unreacted reactants, followed by drying for 24 hours at 120 °C.

Synthesis of modified mesostructured UiO-66 by ionic surfactant CTABr and benzoic acid (UiO-66-Zr-M)

$ZrOCl_2.8H_2O$ (6.44 g), H_2BDC (3.32 g), benzoic acid (4.88 g), HCl (3.2 ml) were dissolved in 250 ml DMF. Subsequently, modulator CTABr (0.365 g) dissolved in 95 ml DMF was added to the mix, stiring until cleared solution obtained, then the mix was transferred in to a round bottomed flask 1000ml, which was attached the reflux condenser, heated at 120 °C for 24 hours with continously stiring 300 rpm. After cooling down to room temperature, the pre-cipitate was collected by centrifugation and washed with DMF three times. Then the solid was stirred in DMF at 90 °C for 12 h, then in methanol at 70 °C for 12 h to remove unreacted chemicals and solvent. The resulting white powder was dried under vacuum at 150 °C for 12 h.

Characterizations

X-ray diffration (XRD) data were recorded using a 8D Advance Bucker diffractometer with CuKα radiation, the scanning angle with a range of 1-50° 2θ. The IR spectra were recorded from disk-membraned samples (1 %) in KBr pellets by IR spectra photometer. Nitrogen adsorption-desorption isotherms were measured at 77 K using a Micromeritics system after the samples were de-gassed at 200 °C for 4 h. The specific surface area, S_{BET}, was determined by the Brunauer-Emmett-Teller (BET) method, and the pore-diameter distribution was analyzed by the Barrett-Joyner-Halenda (BJH) method. Transmission electron micrographs (TEM) were obtained using a JEOL JEM 1230 microscope operating at 80 kV. Diffuse reflectance UV-Vis spectra was recorded in the range of 200-800 nm at room temperature by GBC Instrument-2885. Energy-dispersiveX-ray spectroscopy (EDX). All characteristics of materials in this article were determined at Vietnam Academy of Science and Technology.

Photocatalytic degradation of Chlopyrifos ethyl under simulated sunlight

In each experiment using 30 mg material and 100ml of chlopryrifos ethyl (50 mg/L) solution were put in a glass vessel 250 ml volumme, stiring at 600 rpm in dark for 60 minutes for absorption equilibrium. Then reactions mix was irradiated by Osram lamp Ultra-vitalux 300W (λ = 365-450 nm), keep continuously stirring and taking liquid samples at 90, 120, 150, 180 and 240 minutes. Filtering liquid samples by filter for analysis by UV-Vis spectra at 229 nm.

Reaction constant

Assuming that photochemistry reaction is first- order reaction, reaction constant is calculated by this equation: $-\ln(C_t/C_0) = k.t$; k - constant metabolic reaction rate; C_0 (mg/L): the initial concentrations of chlopryrifos ethyl; C_t (mg/L): the equilibrium concentrations of the adsorbate; V (L): the volume of reaction solution; m (g): the mass of the carrier; k (min^{-1}): reaction constant.

Results and Discussion

Characterifications of samples

The characteristic diffraction peaks at 2θ ~ 6.5°, 8.5° are presented in UiO66, UiO66-A and UiO66-M samples, indicating the formation of crystals. Thus, the structure of UiO-66 is retained after the introduction of defects, in accordance with the XRD analysis. The XRD spectrum of the UiO-66-M sample are diffracted at the angles smaller than 1° which demonstrate the mesopore structure in comparision to UiO66 and UiO66-A. The characteristic peaks of H_2BDC at 17.4°, 25.4°, 28.1° do not appear, which means H_2BDC used in synthesizing process was removed completely.

The IR spectrum showed: the absorption band at frequencies of 1577-1580 cm^{-1} and 1398 cm^{-1} are associated with the OCO asymmetric and symmetric stretch vibrations of the carboxylate groups of the BDC linker.[21] The absorption band at frequency of 1506 cm^{-1} is characterizes the vibrations of the C=C bond within the aromatic ring of the BDC linker [21]. The absorption band with small intensity at the frequency of 746-489 cm^{-1} characterizesthe vibrations of the Zr-O bonds. The absorption band at 1158-1017 cm^{-1} characterizes the oscillation of the benzene ring. In addition, the absorption band at frequencies above 3400 cm^{-1} characterizes water molecules in crystals and water molecules that are physically absorbed inside material pores.

From TEM images of samples UiO-66 (b), UiO-66-A (a), UiO-66-M (c) (Figure 2) it could be seen that UiO-66 no defects possessed cubic shape but UiO-66-A (Figure 2a) showed the crystals were damaged a litle caused by acetic acid. While using ionic surface agent CTABr and benzoic acid in initial mix beside defects creations

https://doi.org/10.51316/jca.2021.139

but also mesoporous structures were formed in UiO-66-M. From the BET results, it can be see that only UiO-66-M) plots have hysteresis loop at P/P_0 of 0.7 and 0.6 respectively that characterize for the existence of meso size pores. Whereas, UiO-66, UiO-66-A plots do not have these characterizations due to the fact of these two materials just contain micropore only.

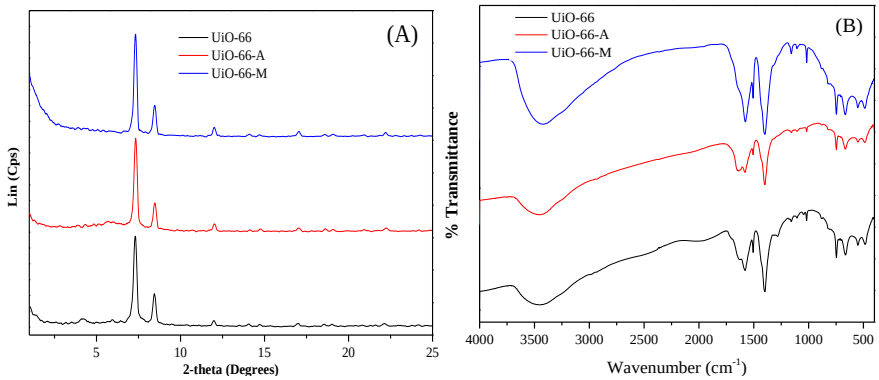

Figure 1: XRD of samples (A), IR of samples (B)

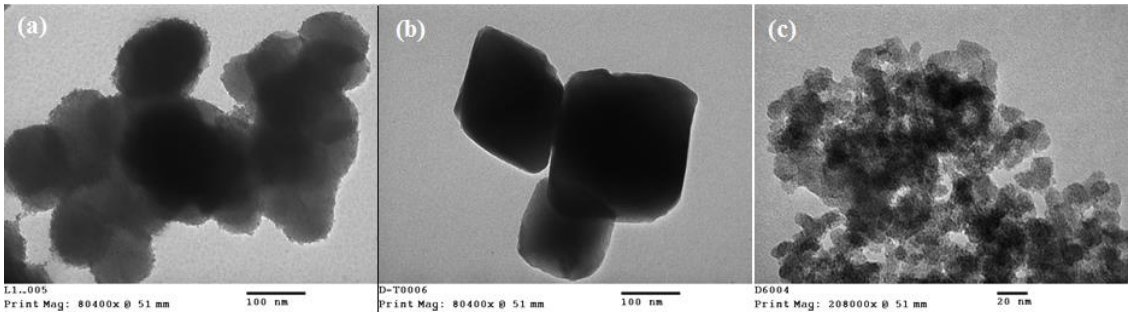

Figure 2: TEM images of samples UiO-66 (b), UiO-66-A (a), UiO-66-M (c)

Table 1: BET parameters of samples

Samples	Modified method	S_{BET} (m^2/g)	V_t (cm^3/g)	d_{pore} (nm)
UiO-66	-	647	0.093	2.18
UiO-66-A	CH_3COOH	1890	0.153	3.09
UiO-66-M	C_6H_5COOH; CTABr	766	1.283	9.26

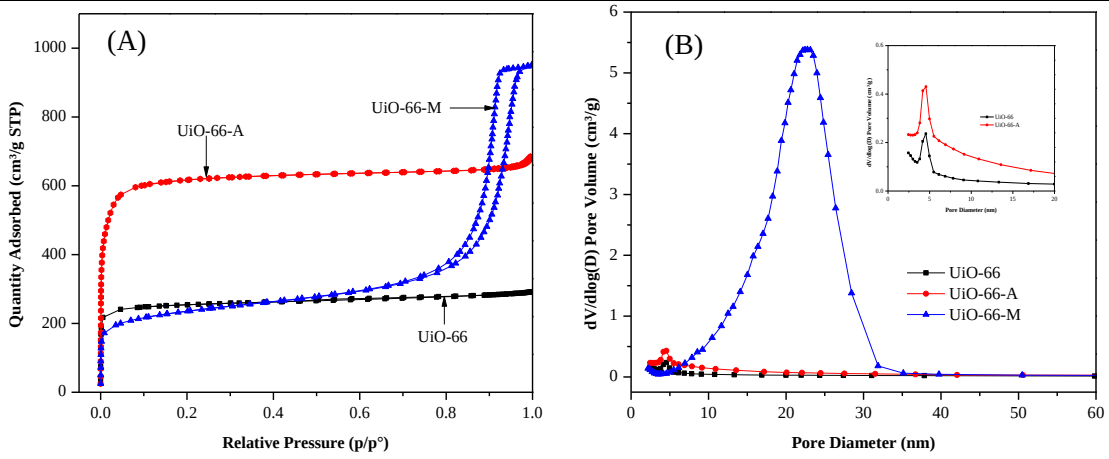

Figure 3: Isothemal absorption/deabsorption nitrogen (A); and pores distribution (B) of samples UiO-66, UiO-66-A, UiO-66-M

https://doi.org/10.51316/jca.2021.139

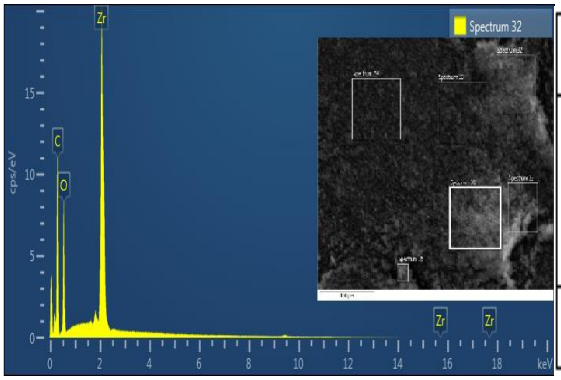

Components	C	O	Zr
% mass	47.47	27.73	24.60
% mol	66.46	29.03	4.52

Figure *4:* EDX and components analysis of UiO-66-M

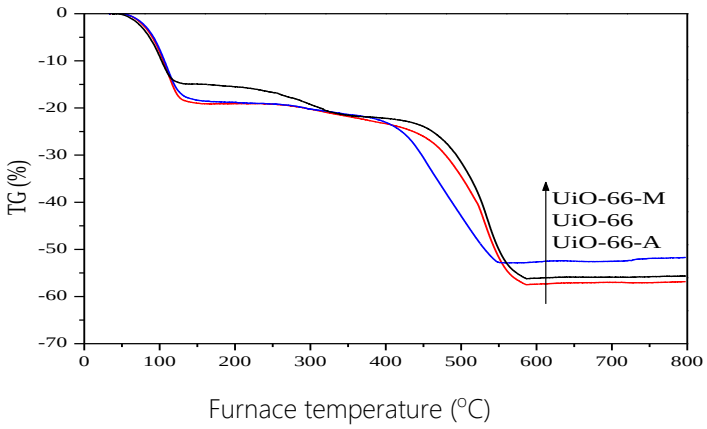

Figure *5:* TGA results obtained of samples samples UiO-66, UiO-66-A, UiO-66-M

Besides that, the big difference in the pore size of UiO-66-M and UiO-66-A may stand for mesostructure ofmaterial. As our results, the creation of defects in UiO-66 framework does not guarantee the enhancement of the BET surface area but increases the pore size, especially intergration mesostructured modification by soft templating (Fig. 3). From TGA results obtained of defected samples it can be seen the thermal stability of the framework is reduced upon the generation of defects (Fig. 5). Both of defective UiO-66-A and UiO66-M showed no improvement adsorption performance for Chlopyrifos because the surface area decreased (table 1). But the existence of supermicropores (UiO-66-A) and mesopores (UiO-66-A) created by linker missing, which allows more active sites accessible to probe molecules or charge change increased the photocatalytic degradation (Fig. 6). Defective UiO-66 UiO-66-A and UiO-66–M showed the rate constants of Photocatalytic degradation of Chlorpyrifos with 2×10^{-4} min^{-1} and 9.1×10^{-3} min^{-1} and 1.23×10^{-2} min^{-1} respectively (Fig 7). Such an improvement was mainly attributed to the pore structure change and additional active sites caused by linker/cluster missing. The selectivity absorption and photocatalyic activeties for decomposition of Chlopyrifos over defected UiO-66-M, UiO-66-A in compared to undefected UiO-66 (figure 6) were mainly caused by the charge change after defecting. It can be explained that when defects are created, especially cluster missing, large pores might be obtained (table 1). Thus exposing more active sites and facilitating diffusion of reactant species and enhance photocatalytic degradation of chlopiryfos can be explained by charge change, whereas the defective sites (missing linkers) playing as vacancy lattice sites, which are incorporated into framework, with stronger π−π bonding contributed to the improved light absorption and reduce the recombinartion of e^-/h^+ both in side and surface of particles materials.[12] For that deffected UiO-66 samples were enhanced Chlopyrifos photocatalytic degradation due to the strong inherent affinity of actieve site and the additional active sites that induced by the change of coordination number.

https://doi.org/10.51316/jca.2021.139

Abosorption and photocatalyticdegradation of chlorpyrifos ethyl in aqueous solution

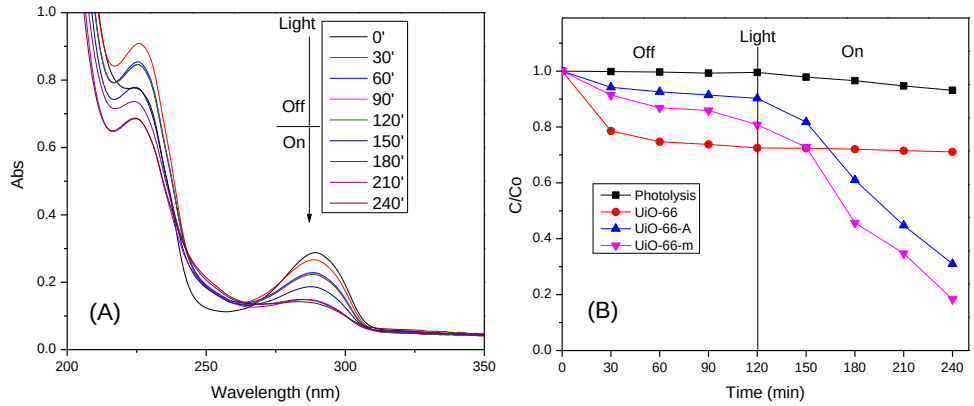

Figure 6: Photocatalytic degradation of Chlorpyrifos over samples UiO-66, UiO-66-A, UiO-66-M (B)

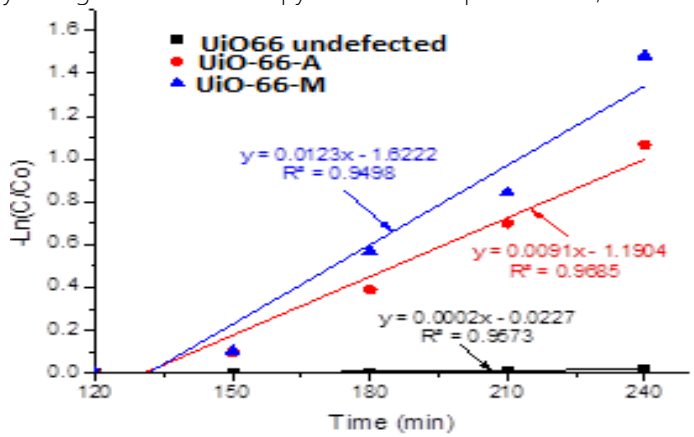

Figure 7: Rate constants of Photocatalytic degradation of Chlorpyrifos for UiO-66, UiO-66-A, UiO-66-M (B)

Table 3: Abosorption capacity and photocatalyticdegradation of chlorpyrifos ethyl in aqueous solution 240 minutes, simulated sunlight 880 mW/cm^2

Samples	Conversion of Chlorpyrifos, % (for 240')	Rate constants of Photocatalytic degradation of Chlorpyrifos Chlorpyrifos (min^{-1})
UiO-66	28.92	2×10^{-4}
UiO-66-A	68.98	9.1×10^{-3}
UiO-66-M	81.65	1.23×10^{-2}

The results of the evaluations of the photodegradation performance of Chlorpyrifos ethyl by the HPLC method (Fig. 8) are also equivalent to the evaluation results of the UV-Vis method analysis (Fig. 6). After 240 min in dark and under simulated sunlight irradation Chlorpyrifos ethyl was decomposed 90 % to non-toxic inorganic with no intermediate componds were presented as showed in the HPLC-MS spectrum.

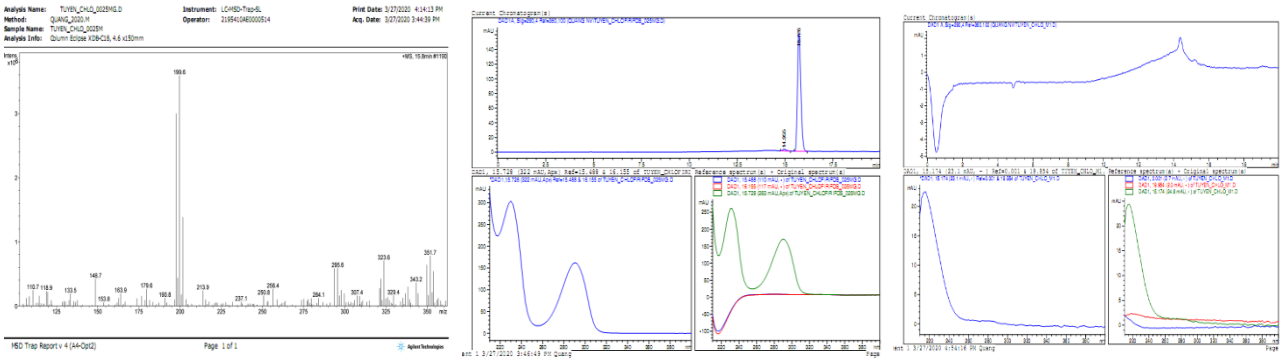

Figure 8: HPLC-MS spectrum of chlorpyrifos and degradation products over photocatalyst UiO-66-M

https://doi.org/10.51316/jca.2021.139

Conclusions

Successfully synthesized modified Metal Organic Framework UiO-66 (Zr) UiO-66, UiO-66-A and UiO-66-M with defects in material network by using surfactant template, acetic acid and benzoic acid as modulators. Defected UiO-66-A and UiO66-M materials showed no improvement adsorption performance but the existence of supermicropores (UiO-66-A) and mesopores (UiO-66-M) created by linker missing, which allows more active sites accessible to probe molecules or charge change increased the photocatalytic degradation of chlopyrifos ethyl in water. The thermal stability of the framework is reduced upon the generation of defects. This is considered as a new point in the methods of synthesis MOFs in general, and also in particular methods of synthesis modified MOFs materials with defects creation combination with intergrated mesostructures, which enhance the photocatalytic degradation of hydrophobic pesticides residues under sun light in agricuture cultivation.

Acknowledgments

This research is funded by Vietnam Academy of Scince and Technology under grant number UDPTCN.06/19-21

References

1. Marco A. Quiroz, Erick R. Bandala and Carlos A. Martínez-Huitle., Fate. 34 (2011) 685-730. https://doi.org/ 10.5772/13597
2. Samreen Heena Khan, Suriyaprabha R., Bhawana Pathakand M. H. Fulekar, Front Nanosci Nanotech. 1(1) (2015) 23-27. https://doi.org/10.15761/FNN.1000105
3. Abedi S., Morsali A., ACS Catal., 4 (2014) 1398-1403. https://doi.org/10.1021/cs500123d
4. Z. Fang, Bueken B., Dirk E. De Vos, and Roland A. Fischer, Angew. Chem. Int. Ed. 54 (2015) 7234-7254. https://doi.org/10.1002/anie.201411540
5. Greig C. Shearer, Sachin Chavan, Silvia Bordiga, Stian Svelle, Unni Olsbye, and Karl Petter Lillerud, Chem. Mater., 28 (2016) 3749-3761. https://doi.org/10.1021/acs.chemmater.6b00602
6. Matthew R. DeStefano, Timur Islamoglu, Sergio J. Garibay, Joseph T. Hupp, and Omar K. Farha., Chem. Mater. 29(3) (2017) 1357-1361. https://doi.org/10.1021/acs.chemmater.6b05115
7. Nguyen Duc Hai, Vu Minh Tan, Dang Huu Canh, Nguyen Dinh Tuyen, Journal of Science and Technology 45 (2018) 86-89.
8. Xiao Feng, Julianna Hajek, Himanshu Sekhar Jena, Guangbo Wang, Savita K. P. Veerapandian, Rino Morent, Nathalie De Geyter, Karen Leyssens, Alexander E. J. Hoffman, Vera Meynen, Carlos Marquez, Dirk E. De Vos, Veronique Van Speybroeck, Karen Leus, and Pascal Van Der Voort, J. Am. Chem. Soc. 142(2020) 3174-3183. https://doi.org/10.1021/jacs.9b13070
9. Yi Feng, Qian Chen, Minqi Jiang, and Jianfeng Yao, Ind. Eng. Chem. Res. 58 (2019) 17648-17659. https://doi.org/10.1021/acs.iecr.9b03188
10. Wenlong Xianga, Jie Rena, Si Chena, Chenyang Shena, Yifei Chena,Minhua Zhanga, Chang-jun Liua, Applied Energy 277 (2020) 115560. https://doi.org/10.1016/j.apenergy.2020.115560
11. Ren J., Ledwaba MV., Musyoka NM., Langmi HW., Mathe M., Liao S., Pang W., Coordination Chemistry Reviews, 349 (2017) 169-197. https://doi.org/10.1016/j.ccr.2017.08.017
12. Katrine L. Svane, Jessica K. Bristow, Julian D. Galeb, Aron Walsh., J. Mater. Chem. A, 6 (2018) 8507-8513. https://doi.org/10.1039/C7TA11155J
13. Matthew R. DeStefano, Timur Islamoglu, Sergio J. Garibay, Joseph T. Hupp, and Omar K. Farha., Chem. Mater. 29(3) (2017) 1357-1361. https://doi.org/10.1021/acs.chemmater.6b05115
14. Aoning Wang, Yingjie Zhou, Zhoulu Wang, Miao Chen, Luyi Sunc and Xiang Liu., RSC Adv. 6 (2016) 3671-3679. https://doi.org/10.1039/C5RA24135A